



University of Kentucky
UKnowledge

Biosystems and Agricultural Engineering Faculty
Publications

Biosystems and Agricultural Engineering

9-2012

Characterizing Physical Properties of Gas-Phase Biofilter Media

Guilherme Del Nero Maia
University of Illinois at Urbana-Champaign

G. Tatiana Sales
University of Illinois at Urbana-Champaign

George B. Day V
University of Kentucky, george.day@uky.edu

Richard S. Gates
University of Illinois at Urbana-Champaign

Joseph L. Taraba
University of Kentucky, joseph.taraba@uky.edu

Right click to open a feedback form in a new tab to let us know how this document benefits you.

Follow this and additional works at: https://uknowledge.uky.edu/bae_facpub

 Part of the [Bioresource and Agricultural Engineering Commons](#)

Repository Citation

Maia, Guilherme Del Nero; Sales, G. Tatiana; Day, George B. V; Gates, Richard S.; and Taraba, Joseph L., "Characterizing Physical Properties of Gas-Phase Biofilter Media" (2012). *Biosystems and Agricultural Engineering Faculty Publications*. 159.
https://uknowledge.uky.edu/bae_facpub/159

This Article is brought to you for free and open access by the Biosystems and Agricultural Engineering at UKnowledge. It has been accepted for inclusion in Biosystems and Agricultural Engineering Faculty Publications by an authorized administrator of UKnowledge. For more information, please contact UKnowledge@lsv.uky.edu.

Characterizing Physical Properties of Gas-Phase Biofilter Media

Notes/Citation Information

Published in *Transactions of the ASABE*, v. 55, issue 5, p. 1939-1950.

© 2012 American Society of Agricultural and Biological Engineers

The copyright holder has granted the permission for posting the article here.

Digital Object Identifier (DOI)

<https://doi.org/10.13031/2013.42356>

CHARACTERIZING PHYSICAL PROPERTIES OF GAS-PHASE BIOFILTER MEDIA

G. D. N. Maia, G. T. Sales, G. B. Day V, R. S. Gates, J. L. Taraba

ABSTRACT. Gas-phase biofiltration is an effective technology for reduction of odors and trace-gas contaminants. Significant contributions to the technical literature regarding the characterization of biofilter media have been generated in the past two decades. Nevertheless, the information produced has not been systematically organized. The objective of this study is to demonstrate and document methods for physical characterization of gas-phase compost biofilters (GPCB). The inclusion of moisture content, compaction, and particle size effects in the determination of media bulk density and porosity, field capacity, drying rate analysis, water sorption isotherms, and resistance to airflow is demonstrated. Results indicated that: (1) higher moisture content led to about 2% reduction in porosity after compaction; (2) biofilter media sieved into three particle size ranges (12.5 mm > PSR1 > 8.0 mm > PSR2 > 4.75 mm > PSR3 > 1.35 mm) produced significantly different media field capacities, i.e., 52.8% (PSR1), 61.6% (PSR2), and 72.2% (PSR3) on a wet basis; (3) a drying rate analysis provides important information regarding media-water relations and can be potentially used for in situ indirect media moisture monitoring (as shown in previous work, changes in drying rate significantly affected ammonia removal and nitrous oxide generation); (4) the Henderson isotherm can be accurately used for dry organic media to determine the minimum moisture required for microbial activity; and finally (5) the combination of high airflow and high moisture content drastically increased pressure drop up to 65-fold (6350 Pa m⁻¹) compared to the lowest pressure drop (98 Pa m⁻¹). Further, the research community should integrate efforts to elaborate standard methods and protocols for physical characterization of gas-phase biofilter media before and during biofilter operation.

Keywords. Biofiltration, Drying rates, Isotherms, Moisture content, Particle size, Porous media.

Physical characterization of gas-phase biofilter media can be used as a management tool for improved biofilter design and for process intervention during biofilter operation. Significant contributions to the topic can be found in the literature. They include critical information regarding selection of media, media particle sizes, moisture levels, and their effects on pressure drop (Maia et al., 2011a; Yang et al., 2011; Dorado et al., 2010; Pantoja Filho et al., 2010; Dumont et al., 2008; Maestre et al., 2007; Nicolai et al., 2006; Nicolai and Lefers, 2006; Nicolai and Schmidt, 2004; Nicolai and Janni, 2001a, 2001b). However, the amount of information developed over the past two decades has not

been systematically organized. Development, selection, and adoption of key physical parameters for improved biofilter design and performance are needed.

MEDIA SELECTION

Compost biofilters are made of organically stable (ideally) materials produced with a combination of organic wastes (active ingredients) such as manure, soil, yard waste, and food waste. Bulking agents are added to the active ingredients to increase porosity and lower pressure drops during the process of composting and to allow the finished material to fully stabilize and mature through a curing process (EPA, 2008). Bulking agents include wood chips, sawdust, hay, straw, pine wood shavings, cardboard, leftover cattle feed, wheat residue pellets, leaves, tobacco stalks, and many others. Seasonal availability of compost ingredients increases the variability of the finished product and its suitability for use in biofilters. Proper biofilter operation requires knowledge of the physical, chemical, and biological properties of compost. Ideally, every batch of new material used in a biofilter would be subjected to careful characterization before its utilization as biofilter media. An attempt to standardize procedures for composting and compost characterization is provided by the U.S. Composting Council (USCC, 2002). While the USCC test methods provide certain media characterization protocols, they lack details that are important for application to gas-phase biofilters, such as moisture control. Further clarification is needed concerning compost quality control as applied to biofilters.

Submitted for review in January 2012 as manuscript number SE 9600; approved for publication by the Structures & Environment Division of ASABE in September 2012.

The authors are **Guilherme D. N. Maia, ASABE Member**, Postdoctoral Researcher Associate, and **G. Tatiana Sales, ASABE Member**, Postdoctoral Research Associate, Department of Agricultural and Biological Engineering, University of Illinois at Urbana-Champaign, Urbana, Illinois; **George B. Day V, ASABE Member**, Research Specialist, Department of Biosystems and Agricultural Engineering, University of Kentucky, Lexington, Kentucky; **Richard S. Gates, ASABE Fellow**, Professor, Department of Agricultural and Biological Engineering, University of Illinois at Urbana-Champaign, Urbana, Illinois; and **Joseph L. Taraba, ASABE Member**, Extension Professor, Department of Biosystems and Agricultural Engineering, University of Kentucky, Lexington, Kentucky. **Corresponding author:** Guilherme D. N. Maia, Department of Agricultural and Biological Engineering, 1304 W. Pennsylvania Avenue, University of Illinois at Urbana-Champaign, Urbana, IL 61801; phone: 859-608-7570; e-mail: gdnmaia@gmail.com.

MEDIA PARTICLE SIZE

Media particle size variability can be substantially reduced through sieving; however, the use of unsieved compost is a common field practice. The selection of particle size ranges can potentially improve the characterization of a batch of compost, especially compost-moisture interactions over different proportions or ratios. Media particles vary substantially in size, which affects medium characteristics such as resistance to airflow and total biofilm surface area (Devanny et al., 1999). Particle size can also impact oxygen distribution within biofilter media. The majority of gas-phase biofilters operating in the field are designed to work aerobically. Nevertheless, media aggregates may develop mixed anoxic/anaerobic zones in microaerophilic environments. Aggregates >10 mm in diameter often have anaerobic zones (Sexstone et al., 1985), and aggregates as small as 4 mm can potentially develop anaerobic zones (Maia et al., 2012).

POROSITY AND RESISTANCE TO AIRFLOW

Bed porosity is a critical parameter related to the resistance to airflow through media. It can be defined as the ratio of the pore volume to the total volume occupied by the material. Similar materials with different bed porosities can result in large pressure drop differences (Yang et al., 2011). It is recommended to include the effects of bed porosity on pressure drop in media characterization protocols (Sales, 2008; Liberty, 2002). In addition to bed porosity, pore distribution is also an important parameter not commonly used in the evaluation of biofilter media. Levin et al. (2007) showed that substantial changes in pore distribution occurred for a two-week biodegradation of wood chips, while only small changes in bed porosity were observed. Changes in pore distribution are more likely to affect biofilter media microbial dynamics than media pressure drop. Biofilters will probably remain effective for 3 to 10 years (or more) before considerable pressure drop increase is observed (Nicolai and Lefers, 2006).

Nicolai and Janni (2001a) compared mixtures of compost and wood chips and reported that pressure drop increased and porosity of the mixture decreased as the amount of compost in the media mixture increased. Sadaka et al. (2002) compared wood chips and wood mulch as bulking agents and reported that mulch had lower porosity than chips for the same compost to bulking agent ratio, thus providing higher resistance to airflow. Morgan-Sagastume et al. (2003) reported that small pore diameters with high connectivity (wide conduit network) improved biofilter performance, as the contact between the flowing gas and media increased. Nicolai and Janni (2001b) reported that higher percentages of compost by weight in media improved odor reduction and removal of hydrogen sulfide (H_2S) and ammonia (NH_3). Bed porosity data should be combined with moisture content when determining their effects on pressure drop (Sales, 2008; Liberty, 2002).

MOISTURE MONITORING

Poor moisture control is the main cause of biofilter failure (Nicolai and Lefers, 2006). The procedures for charac-

terizing gas-phase compost biofilter (GPCB) media should include moisture effects. In the field, continuous monitoring of media moisture conditions during the process of biofiltration is a complex task with very few proven cases of success (Dutra de Melo, 2011; Nicolai and Lefers, 2006; Funk et al., 2005). Oversaturation of media with water is one commonly used approach to maintain contaminant sorption and microbial consumption of the contaminant. However, saturation can potentially generate sub-products, such as nitrous oxide (N_2O) and methane (CH_4) in compost biofilters treating NH_3 (Maia, 2010; Maia et al., 2011b; Maia et al., 2012). The identification of drying stages (with the continuous monitoring of inlet-outlet humidity levels) is a practical alternative to determine GPCB media moisture conditions. Maia (2010) showed that different drying stages significantly affect biofilter removal efficiency and fate of contaminants. The classical but to date unused tool to determine moisture conditions from different stages of drying is the drying rate versus moisture content curve. The curve is characterized for the media prior to biofilter operation. The full spectrum of moisture from saturated media to dry equilibrium media can be obtained and related to the corresponding drying rate stage. During biofilter operation, only air temperature and humidity need to be monitored using affordable T/RH sensors placed at the biofilter inlet and outlet. Drying rates can then be accurately related to the moisture content levels obtained from the drying rate versus moisture content curve before operation. The procedure allows indirect but continuous monitoring of moisture.

Foust et al. (1964) presented the drying process for relatively stable conditions of temperature and humidity (fig. 1a). The general drying pattern is divided into four stages. The initial unsteady stage (segment AB in fig. 1a) is marked by temperature and drying rate fluctuations in the solid media after first contact with the drying gas. The shape of segment AB is typical; however, it can assume any shape (including decreasing drying rate). Secondly, the constant drying rate stage (segment BC in fig. 1a) occurs when most of the solid surface is saturated with water and the porous solid does not directly influence the drying process. The rate controlling factors in the constant drying rate stage are: (1) the diffusion of water vapor across the air-moisture interface, and (2) the rate at which moisture is removed from the media surface (Mujumdar and Menon, 1995). The drying rate is constant up to a transitional point (point C in fig. 1a) that corresponds to the critical moisture content of the material. At the critical moisture level, unbound water no longer covers the entire external surface of the solid porous material. Thirdly, the first falling drying rate stage (segment CD in fig. 1a) indicates that internal liquid diffuses to the solid surface at a rate slower than evaporation from the surface. In this drying stage, water vapor movement by diffusion through pores and capillarity are the drying rate controlling factors (Mujumdar and Menon, 1995). Finally, in the second drying rate stage (point D), there is minimal moisture within the internal solid pore surfaces. Beyond point D, bound water and capillary water are predominant in controlling the drying rate until the equilibrium moisture content is finally reached. Moisture equilibrium occurs when the vapor pressure over the solid matches

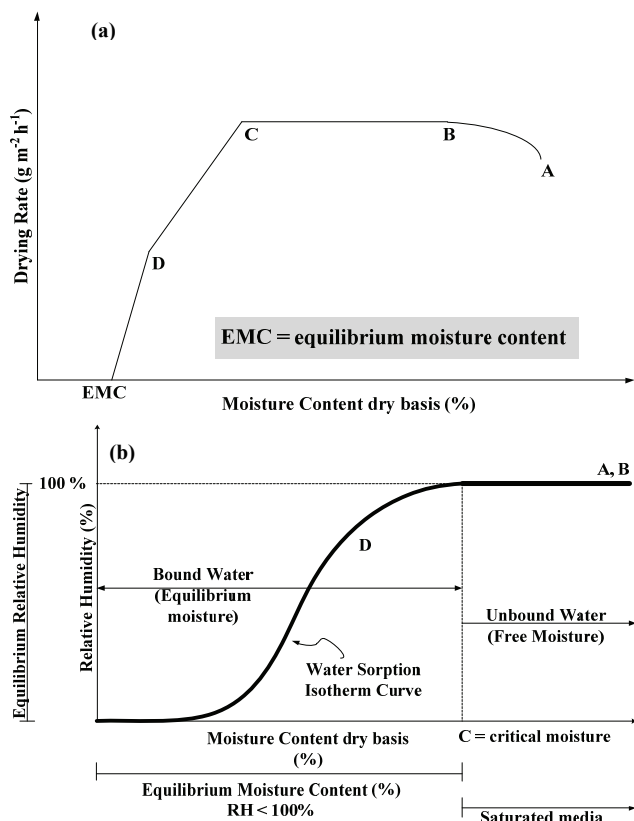


Figure 1. (a) Typical curve of drying rate as a function of moisture content for constant drying conditions (Maia, 2010), and (b) moisture types lower and higher than critical moisture content (modified from Foust et al., 1964).

the water vapor partial pressure of the incoming air stream. Figure 1b illustrates the transition from situations of unbound moisture (free water with high mobility) to bound moisture (low mobility water marked by strong physical-chemical interactions between water molecules and the solid surface). Situations of equilibrium between water vapor and solid media are conveniently described with the use of water sorption isotherms (Maia et al. 2011a) applied for relative humidities below saturation.

WATER SORPTION ISOTHERMS

Equilibrium relative humidity (also called water activity) between the compost material and its surroundings is the determinant that ensures optimum levels of microbial activity after media moisture levels are below a critical threshold (absence of enough mobile free water). Most bacteria struggle to survive in environments with water activity levels lower than 95%. Isotherms are studied for lower levels of moisture in equilibrium with its surroundings. Bound moisture is predominant in these situations and is represented by water that is either (1) loose in chemical combination, (2) present as liquid solution within the solid, or (3) trapped in the microstructure of the solid owing to capillary forces (Mujumdar and Menon, 1995). Maia et al. (2011a) tested seven isotherm models and applied them to four different particle size ranges of compost biofilter media, with the Henderson model providing the best fit with observations. The Henderson isotherm has been extensively

used to describe water sorption behavior of biological materials. The advantage of the original Henderson formulation is the small number of model parameters and frequent high correlation with experimental data. The Henderson equation is described as follows (Henderson et al., 1997; Henderson, 1952):

$$EMC = \left(\frac{-\ln(1-ERH)}{H_1 \times T} \right)^{(1/H_2)} \quad (1)$$

where T is the temperature (K), H_1 and H_2 are empirical constants of the material, ERH is the equilibrium relative humidity (in decimal), and EMC is the equilibrium moisture content (in percent).

Our working hypothesis is that the inclusion of moisture content and particle size in the biofilter media characterization will improve biofilter design and operation. Thus, the objective of this study is to demonstrate and document methods for physical characterization of GPCB. The inclusion of both moisture content and particle size in the determination of media bulk density and porosity, field capacity, drying rate analysis, water sorption isotherms, and resistance to airflow is demonstrated.

MATERIALS AND METHODS

The GPCB media used in this study were sieved into three particle size ranges (12.5 mm > PSR1 > 8.0 mm > PSR2 > 4.75 mm > PSR3 > 1.35 mm) and subjected to the following tests:

- Bulk density and porosity at four levels of moisture content (as-received and 30%, 45%, and 60% wet basis).
- Field capacity.
- Drying rate analysis.
- Water sorption isotherms (PSR3 only).
- Airflow resistance for wet (62% to 65% w.b.) and dry (5.5% to 6.8% w.b.) media (PSR3 only).

BIOFILTER MEDIA SOURCE

Compost material used as biofilter media was collected from the University of Kentucky Animal Research Center, located in Versailles, Kentucky. Active ingredients used as compost material included horse manure, cattle manure, and chicken waste. Bulking agents were added to these organic ingredients to improve aeration. Bulking agents primarily included wood chips (usually available throughout the year), sawdust, leaves, ground hay, tobacco stalks (seasonal), gray hay, and others. Further details about the preparation, cure, and selection of biofilter media can be found in Dutra de Melo (2011), Maia (2010), and Sales (2008). The selection of PSR3 for airflow resistance testing is justified by Maia et al. (2011a).

PARTICLE SIZE DISTRIBUTION

As-received samples of compost (902 g ±83 g or 3125 mL) were sieved in a testing sieve shaker (Ro-Tap model B, W. S. Tyler, Inc., Mentor, Ohio) for 2 min using

12.5 mm, 8.0 mm, 4.75 mm, and 1.35 mm screens. The amount of compost retained by each screen was poured into a beaker and its bulk volume determined.

BULK DENSITY, PARTICLE DENSITY, AND POROSITY

Bulk density of each particle size range ($n = 3$) was determined by pouring 50 g of as-received compost into a graduated cylinder and the initial undisturbed volumes were determined. Each cylinder was then vibrated (Dr. Scholl's Model DR7565, Schering-Plough HealthCare Products, Inc., Kenilworth, N.J.) for 30 s and the compacted volumes were measured. In order to determine bulk density at different moisture contents, each sample was removed and mixed with water, poured back into the cylinder, and its volume measured before and after vibration. The amount of water to be added was determined according to the initial and desired moisture contents (30%, 45%, and 60% w.b.). The amount of water required to achieve the desired initial moisture content was determined using equation 2:

$$m_{added} = \left(\frac{MC_{desired}}{1 - MC_{desired}} - MC_{as-received} \right) \times m_{compost} \quad (2)$$

where m_{added} is the mass of water needed to reach the desired moisture content (g), $MC_{desired}$ is the desired moisture content (w.b., decimal), $MC_{as-received}$ is the moisture condition of the compost when collected (w.b., decimal), and $m_{compost}$ (g) is the mass of the as-received compost used.

Compost particle density was determined by pouring 20 g of each particle size range of as-received compost into three graduated cylinders and adding methanol from a 150 mL container to each cylinder up to the 150 mL mark (Liberty, 2002). Methanol occupied the void spaces of the material, and the remaining volume of methanol represented the volume of particles. Porosity was determined for each particle size range from the results of bulk and particle density by using equation 3 (Pushnov, 2006):

$$\varepsilon = \left(1 - \frac{\rho_b}{\rho_p} \right) \times 100 \quad (3)$$

where ε is the overall porosity (%), ρ_b is bulk density (g cm^{-3}), and ρ_p is the particle density (g cm^{-3}).

BIOFILTER MEDIA FIELD CAPACITY (MFC)

Samples of as-received compost (30 g each) at known initial moisture content were saturated with water, stirred for 3 min, and left to rest for 7 min to absorb water. Next, the saturated compost was poured into three Buchner funnels on top of Erlenmeyer flasks, covered with parafilm, and taken to an environmental chamber at 25°C and 58% RH, where they were drained for 4 h. Finally, the drained compost was weighed, dried in an oven for 24 h at 100°C, and weighed again after oven drying for determination of MFC.

DRYING RATE ANALYSIS

Samples of particle sizes PSR1, PSR2, and PSR3 were dried inside a T/RH controlled environmental chamber (Parameter Generation and Control, Black Mountain, N.C.) for 20 days using 4 L min^{-1} airflow at 25°C and 58% RH (fig. 2). Air RH = 58% (unsaturated air; dew point = 16°C) was used to represent typical barn exhaust RH values. The initial media moisture contents (w.b.) for PSR1, PSR2, and PSR3 were 52.8%, 61.6%, and 72.2%, respectively, which represents the MFC of the material. The amount of water required to achieve desired initial moisture content was determined using equation 2. The compost-water mixtures from PSR1, PSR2, and PSR3 were placed inside 2.7 L Scienceware containers (model 42010, Bel-Art Products, Wayne, N.J.), and the process was replicated three times. Compost water loss and water loss rates were determined by recording the weight daily for 20 days. Daily drying rate ($\text{g H}_2\text{O h}^{-1}$) was computed for each 24 h interval. The daily drying rate versus moisture content (% w.b.) curve was then constructed for evaluation of media moisture conditions. Data were divided into three drying stages: constant drying rate stage, first falling drying rate stage, and second falling drying rate stage, per figure 1. The stages were

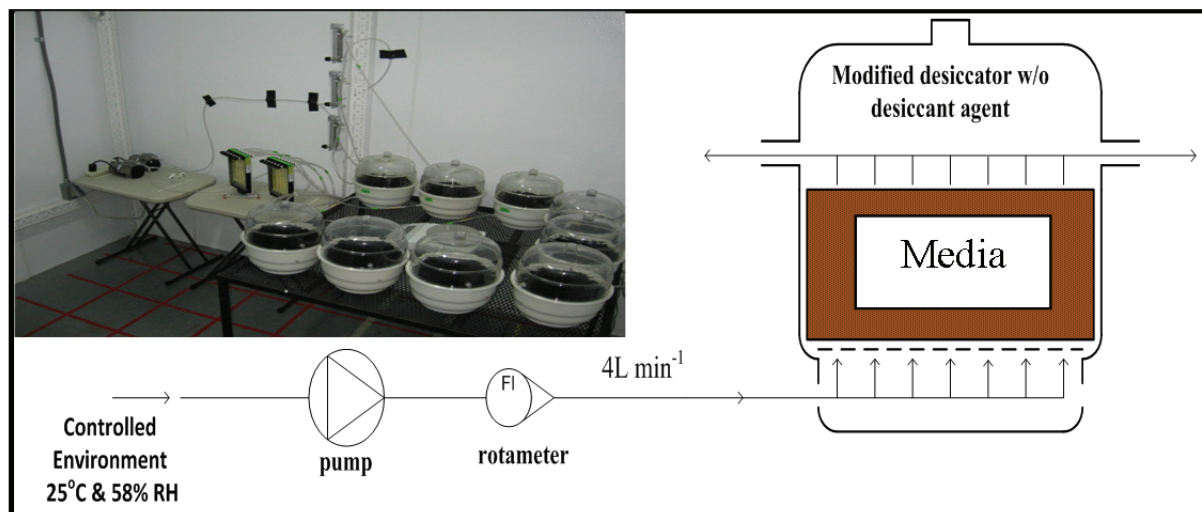


Figure 2. Schematic for determination of the moisture curve.

defined with comparisons between linear regression slopes from moving clusters of successive observation points. The biggest changes between slopes were considered to be drying rate stage transitions (second-derivative method). Finally, linear regressions were applied for the three drying rate stages with slopes evaluated with a t-test (SigmaPlot, version 10.0., Systat Software, Inc., Chicago, Ill.).

EVALUATION OF ISOTHERMS

A methodology was applied to determine compost media water sorption isotherms using the Henderson (1952) equation as developed by Maia et al. (2011a). Isotherms for four particle size ranges within PSR3 (4.76 mm > PSR3-1 > 3.36 mm > PSR3-2 > 2.38 mm > PSR3-3 > 2.00 mm > PSR3-4 > 1.68 mm) were fitted to equation 1 by nonlinear regression (SigmaPlot, version 10.0., Systat Software, Inc., Chicago, Ill.). The best goodness-of-fit was used as the criterion to evaluate differences among particle size ranges. The best model was used for predictions based on confidence intervals of the regression and new observations (prediction intervals). Samples were placed in a controlled environmental chamber (Parameter Generation and Control, Black Mountain, N.C.) with fixed temperature (25°C) while varying the relative humidity from 45% to 55%, 65%, 75%, 85%, 95%, and 99%. Initial relative humidity was set at 45% in the environmental chamber, and one day was allowed for the chamber to reach equilibrium. Relative humidity was increased every five days. Compost sample moisture contents were measured inside the environmental chamber by weighing the samples with a digital scale.

AIRFLOW RESISTANCE OF WET AND DRY MEDIA

A quarter-scale model biofilter (fig. 3) was used to determine the airflow resistance of the media. The model biofilter internal area was 1.00 m × 0.60 m, and it was loaded with loose compost up to a height of 0.46 m. The base was a molded plastic plenum (BioAer, BacTee Systems, Inc., Grand Forks, N.D.) used in potato storage structures. Media for these tests were obtained using similar screen sizes as used in the particle size characterization tests, although using a custom-fabricated shaker platform.



Figure 3. Biofilter used for preliminary pressure drop tests.

Eight holes (four rows and two columns), vertically spaced 12.7 cm apart, were drilled in the back wall of the model biofilter, which was loaded with 0.27 m³ ±2.2% of dry compost (10.6% ±0.13% w.b.) in size range PSR3 to a height of 45.7 ±1.0 cm. The smaller particle size range (PSR3) was chosen because it provided the highest resistance to airflow of the three ranges evaluated. Vibration was applied to the biofilter with an air hammer for 30 s on each of 16 different points (four on each side wall and eight on the back) for a total of 8 min. Vibration allows rearranging of the particles for homogenization of the bulk density and for repeatability of the procedure. After vibration, the compost column height dropped from 45.7 ±1.0 cm to 40.6 ±1.0 cm, changing its bulk density from 237.5 to 266.7 kg m⁻³.

A digital manometer (model 475, Dwyer Instruments, Inc., Michigan City, Ind.) was used to record pressure differences (positive pressure within the compost column – atmospheric pressure) along the eight ports on the back wall of the biofilter. Readings from the same row were averaged, yielding four pressure measurements along the vertical direction. Pressure differences between vertical increments were used to describe the pressure drop profile along the compost column. Pressure differences between the plenum and the first row of ports included pressure drop along the first layer of compost and also across the aeration floor slots. Superficial air velocity was adjusted over a range of 59 to 1770 m³ h⁻¹ m⁻² of medium by means of a ventilation chamber (ASHRAE, 1999). The ventilation chamber was comprised of a blower (Dayton 4C131, 13.5 in., 2 hp, Grainger, Inc., Lake Forest, Ill.), ten calibrated flow nozzles with diameters varying from 1.3 to 15.2 cm, and two standard liquid manometers (model 424, Dwyer Instruments, Inc.), one upstream and one downstream of the nozzles. Actual airflow rates were calculated according to the pressure loss across the calibrated nozzles. Four runs were performed, two each with dry compost (5.5% and 6.8% w.b.) and wet compost (61.9% and 64.9% w.b.). In the latter tests, water was added until drainage occurred (soaked medium). Once excessive water was drained, the wet compost samples were taken for determining wet medium moisture content, and pressure drop testing was carried out.

RESULTS AND DISCUSSION

PARTICLE SIZE DISTRIBUTION

Particle size ranges PSR1, PSR2, and PSR3 together comprised 51.4% ±4.6% of the total volume, while coarser material represented 2.3% ±0.9% and finer material represented 46.3% ±1.9% by volume (fig. 4). This considerable volume of fines can negatively affect biofilter performance in the field (Devinny et al., 1999). For instance, finer particles tend to aggregate and increase media pressure drop as well as flow channeling. High pressure drops increase biofilter energy requirements, with increased operation costs.

BULK DENSITY, PARTICLE DENSITY, AND POROSITY

Particle densities, bulk densities, and porosities before and after vibration of the material at different moisture contents are shown in table 1. Material vibration and water ad-

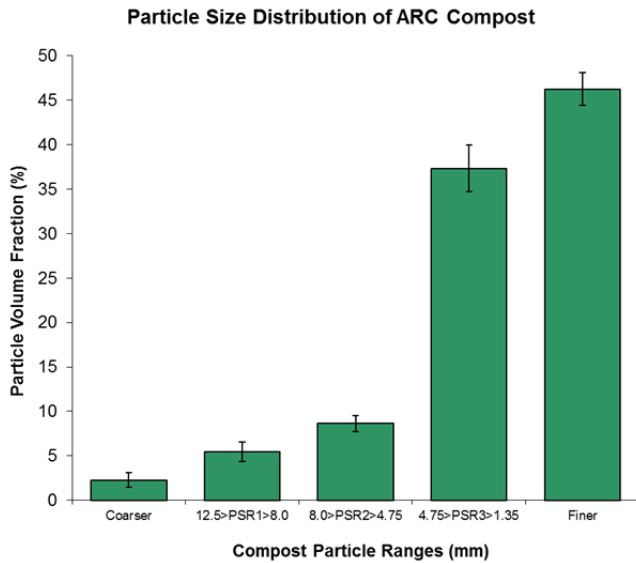
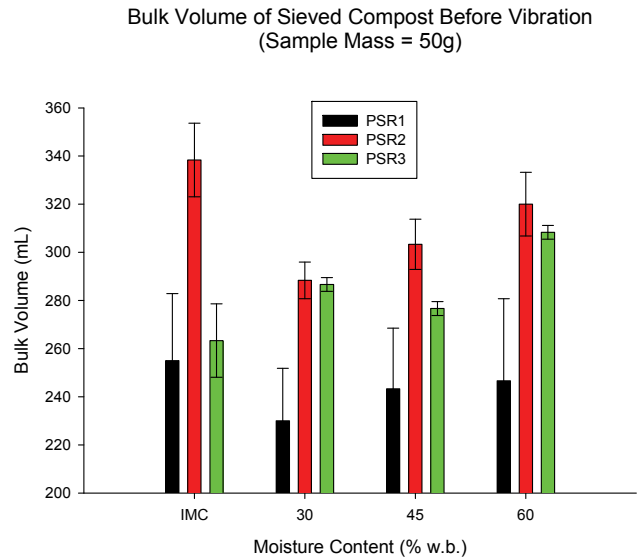


Figure 4. Particle size distribution where PSR1, PSR2, and PSR3 comprise respectively 5.5% ($s = 1.1$), 8.6% ($s = 0.9$), and 37.4% ($s = 2.6$) of the total amount sieved. Error bars represent standard deviations (s) for three samples ($n = 3$).

dition resulted in different particle density characteristics among the three particle size ranges. Both vibration of and water addition to the as-received samples restructured the media mixture. PSR2 exhibited an initial reduction in porosity and increase in bulk density with water addition both before and after vibration. By contrast, PSR3 did not exhibit any reduction in porosity or increase in bulk density (fig. 5). This behavior was potentially caused by particle shape. PSR2 particles were mostly wood chips with an elongated shape, whereas PSR3 particles were mostly flake-shaped mulch. Thus, one hypothesis to explain this phenomenon is that elongated wood chips stack when poured in such a way that large void spaces are created. Hence, both vibration and water addition rearrange the elongated wood chips, filling most of these large void spaces and resulting in a bulk density increase. On the other hand, flake-shaped mulch particles tend to fill the spaces at pouring. Thus, vibration or water addition may not restructure the PSR3 material by much. Vibration reduced PSR1 porosity by 8.4% and 2.4% for initial moisture content of



Bulk Volume of Sieved Compost After Vibration (Sample Mass = 50g)

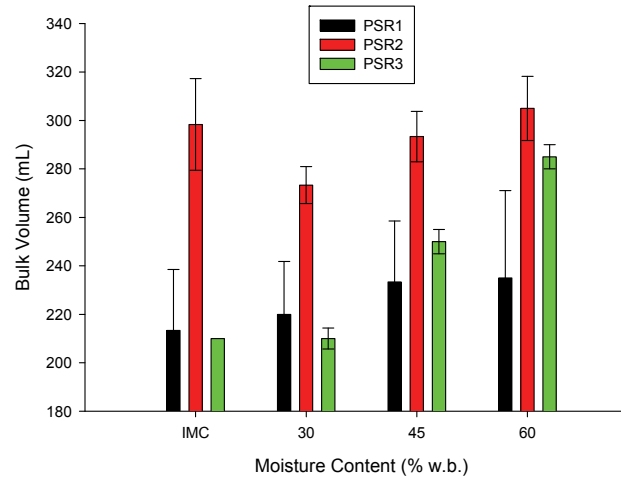


Figure 5. Bulk volume of different compost particle size ranges (12.5 mm > PSR1 > 8.0 mm > PSR2 > 4.75 mm > PSR3 > 1.35 mm) and moisture contents before (top) and after (bottom) vibration of material. IMC = initial moisture content (as-received material).

Table 1. Bulk density before (BDBV) and after (BDAV) vibration of compost sample, particle density (DP), and porosity before (PBV) and after (PAV) vibration of each compost particle size range, as well as standard deviations ($n = 3$).

Analysis	Range	As-Received	30% w.b.	45% w.b.	60% w.b.
BDBV (g cm^{-3})	1	0.20 \pm 0.02	0.24 \pm 0.03	0.22 \pm 0.02	0.23 \pm 0.02
	2	0.15 \pm 0.01	0.17 \pm 0.01	0.17 \pm 0.01	0.18 \pm 0.01
	3	0.19 \pm 0.01	0.24 \pm 0.00	0.17 \pm 0.00	0.24 \pm 0.01
BDAV (g cm^{-3})	1	0.21 \pm 0.02	0.22 \pm 0.02	0.21 \pm 0.03	0.22 \pm 0.03
	2	0.17 \pm 0.01	0.17 \pm 0.01	0.16 \pm 0.01	0.16 \pm 0.01
	3	0.18 \pm 0.00	0.20 \pm 0.00	0.16 \pm 0.00	0.18 \pm 0.00
DP (g cm^{-3})	1	0.66 \pm 0.01	-	-	-
	2	0.78 \pm 0.08	-	-	-
	3	0.85 \pm 0.07	-	-	-
PBV (%)	1	70.10 \pm 3.70	66.93 \pm 3.40	68.69 \pm 3.80	68.95 \pm 4.50
	2	80.86 \pm 1.10	77.53 \pm 1.80	78.65 \pm 1.50	79.77 \pm 1.20
	3	77.60 \pm 0.70	79.39 \pm 2.00	78.65 \pm 2.00	80.83 \pm 1.90
PAV (%)	1	64.20 \pm 4.70	65.41 \pm 3.70	67.32 \pm 4.00	67.31 \pm 5.20
	2	78.30 \pm 0.80	76.30 \pm 1.90	77.92 \pm 1.60	78.77 \pm 1.20
	3	71.87 \pm 2.50	71.83 \pm 3.10	76.35 \pm 2.50	79.26 \pm 2.20

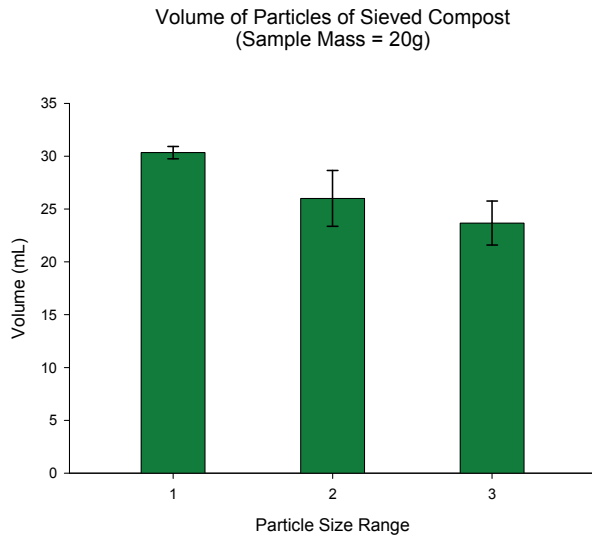


Figure 6. Volume of particles of different compost particle sizes ranges (12.5 mm > PSR1 > 8.0 mm > PSR2 > 4.75 mm > PSR3 > 1.35 mm).

15.4% and 60% w.b., respectively. Vibration reduced PSR2 porosity by 3.2% and 1.3% for initial moisture content of 17.7% and 60% w.b., respectively. Finally, vibration reduced PSR3 porosity by 7.4% and 1.9% for initial moisture content of 19.9% and 60% w.b, respectively (table 1). For the same sample size (20 g) of sieved compost material, PSR1 contained 30.3 ± 0.6 mL of particles, whereas PSR2 and PSR3 contained 26 ± 2.7 mL and 23.7 ± 2.1 mL of particles, respectively. Thus, PSR1 is comprised of the least dense particles, which are mostly plant stalks and wood chips (fig. 6).

BIOFILTER MEDIA FIELD CAPACITY

Media field capacities (moisture content, % w.b.) were 52.8% (PSR1), 61.6% (PSR2), and 72.2% (PSR3). As expected, the smaller particle size range (PSR3) was able to hold more water. These results were used to determine the amount of moisture that could be added to each particle size range to reach its water capacity without becoming waterlogged, which could cause excessive drainage after loading of the GPCB.

EVALUATION OF WET MEDIA: DRYING RATE VERSUS MOISTURE CONTENT CURVE

Moisture content (% w.b.) versus time was generated ($n = 3$; fig. 7a) together with the drying rate versus moisture content curve ($n = 3$; fig. 7b) for PSR1, PSR2, and PSR3. Results are for drying conditions set at 4 L min^{-1} , 25°C , and 58% RH (fig. 2).

Constant Drying Rate

The linear curve adjusted to the observations in the constant drying rate period had zero slope for PSR1 ($p = 0.6032$; $r^2 = 0.0477$), PSR2 ($p = 0.8513$; $r^2 = 0.01$), and PSR3 ($p = 0.7437$; $r^2 = 0.0061$), comprising the moisture content range of 34% to 51% (PSR1), 43% to 61% (PSR2), and 48% to 71% (PSR3) (w.b.) (table 2). The constant drying rate period corresponds to the linear range of the moisture versus time curve that occurred during the first 8-day

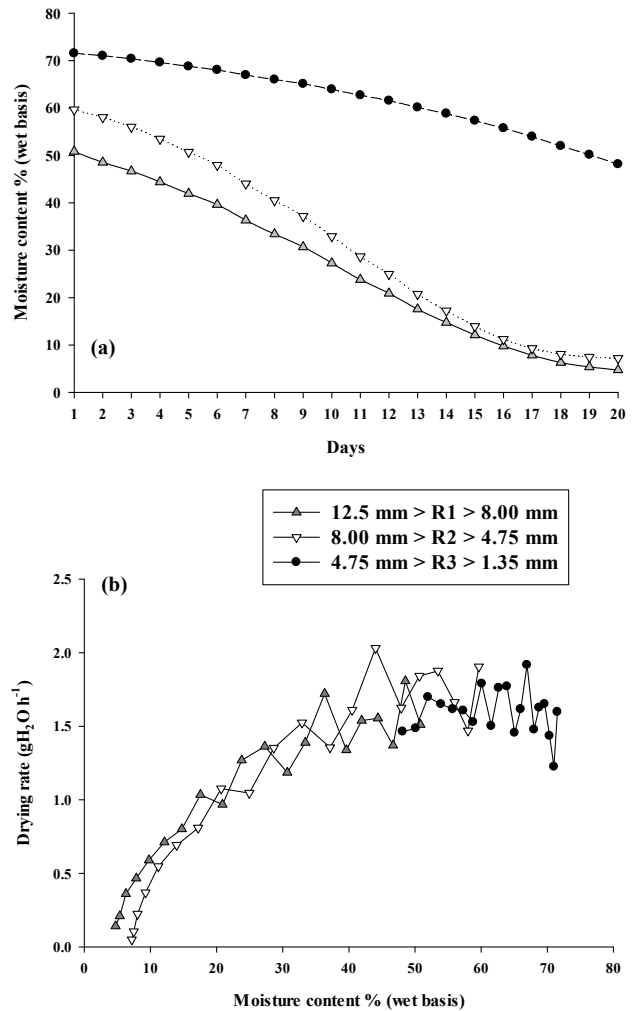


Figure 7. (a) Moisture content versus time, and (b) drying rate versus moisture content.

period for PSR1 ($1.5 \text{ g H}_2\text{O h}^{-1}$; fig. 8a) and PSR2 ($1.9 \text{ g H}_2\text{O h}^{-1}$; fig. 8b). PSR3 remained in the constant drying rate for the whole duration of the experiment ($1.7 \text{ g H}_2\text{O h}^{-1}$; fig. 8c); thus, a longer drying period would be needed to determine the PSR3 full moisture range. The rate controlling factors in the constant drying rate include diffusion of water vapor across the air-moisture interface and the rate at which the surface for diffusion is removed (Mujumdar and Menon, 1995).

Critical Moisture Range

Critical moisture is hard to define experimentally (Foust et al., 1964). The critical moisture range for this material appeared to be approximately 27% to 33% (w.b.) for PSR1 (fig. 8a) and 39% to 43% (w.b.) for PSR2 (fig. 8b).

First Falling Drying Rate

The drying rate of the first falling drying rate period was $\text{DR} = (0.0437 \pm 0.0047) \times \text{MC} + (0.1752 \pm 0.0864)$ for PSR1 and $\text{DR} = (0.0355 \pm 0.0046) \times \text{MC} + (0.1561 \pm 0.1226)$ for PSR2. This period comprised the moisture content range of 10% to 27% w.b. for PSR1 (fig. 8a) and 13% to 39% w.b. for PSR2 (fig. 8b). The transition from a predominance of unbound surface moisture to a predominance of intersti-

Table 2. Statistical parameters (and standard errors) of linear regressions ($\alpha = 5\%$).

Particle Size Range	Media Moisture Condition	Regression Equation (with Standard Error)	r^2
PSR1	Constant drying rate	$DR = 1.2704 \pm 0.4757$	0.0477
	First falling drying rate	$DR = (0.0437 \pm 0.0047) \times MC + (0.1752 \pm 0.0864)$	0.9721
	Second falling drying rate	$DR = (0.1063 \pm 0.0145) \times MC + (-0.3499 \pm 0.0895)$	0.9642
PSR2	Constant drying rate	$DR = 1.8754 \pm 0.6323$	0.0063
	First falling drying rate	$DR = (0.0355 \pm 0.0046) \times MC + (0.1561 \pm 0.1226)$	0.9086
	Second falling drying rate	$DR = (0.10965 \pm 0.0076) \times MC + (-0.7451 \pm 0.0654)$	0.9904
PSR3	Constant drying rate	$DR = 1.6967 \pm 0.3121$	0.0061

tial/bound moisture occurred in this stage (days 9 to 16, fig. 7a). In this phase, water vapor movement by diffusion and capillarity are the drying rate controlling factors (Mujumdar and Menon, 1995).

Second Falling Drying Rate

The drying rate of the second falling drying rate period was $DR = (0.0437 \pm 0.0047) \times MC + (0.1752 \pm 0.0864)$ for PSR1 and $DR = (0.0355 \pm 0.0046) \times MC + (0.1561 \pm 0.1226)$ for PSR2, comprising a moisture content range of approximately 5% to 8% w.b. for PSR1 (fig. 8a) and 8% to 11% w.b. for PSR2 (fig. 8b). In this stage (days 17 to 20, fig. 7a), inter-

stitial/bound moisture is predominant, and the material is moving toward equilibrium moisture content. The rate controlling factors in this range are (1) heat conduction for materials with low bulk density (external dry zones have low conductivity, and heat transfer to the surface becomes a limiting factor) and (2) diffusion from the particle interior to the surface for materials with high bulk density and small micropores (Mujumdar and Menon, 1995).

Particle size range PSR3 maintained higher levels of MC (>45% w.b.) and remained in the constant drying rate longer than PSR1 and PSR2. In practical terms, this suggests that moisture can be applied between longer intervals

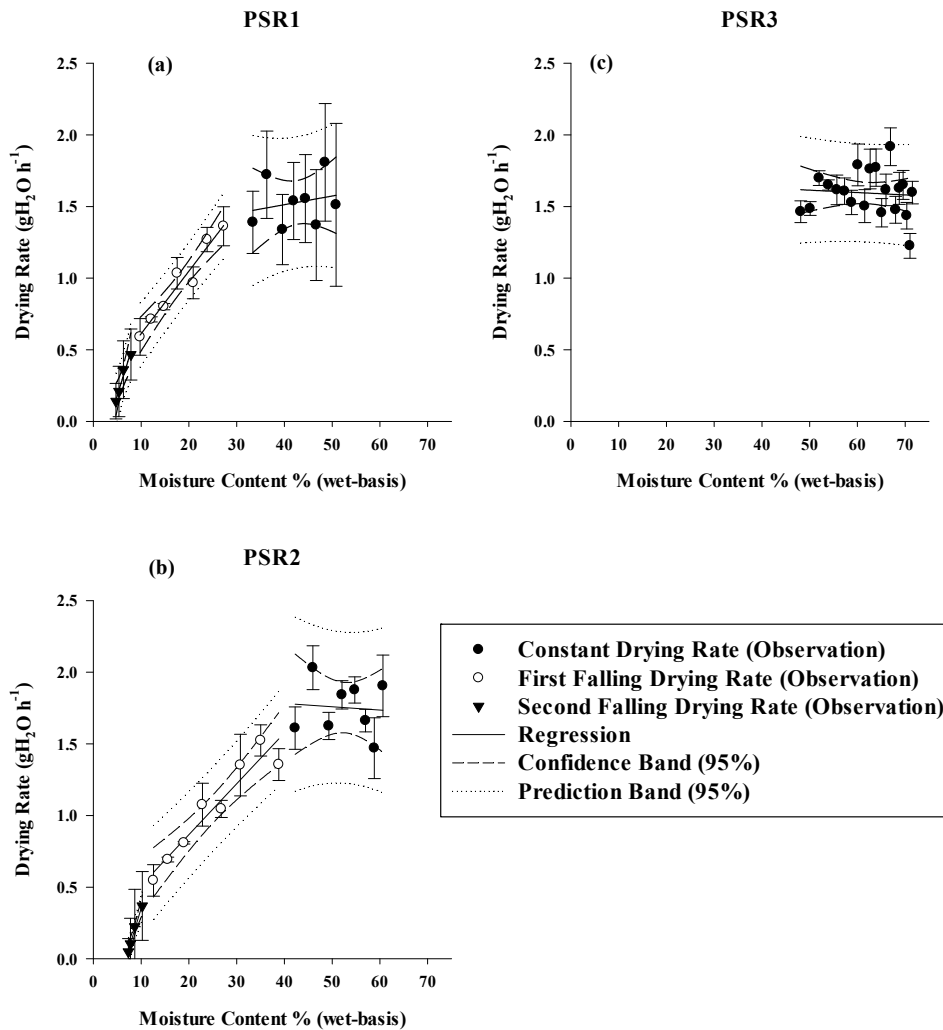


Figure 8. Media moisture condition in the drying rate versus moisture content curve: (a) 12.5 mm > PSR1 > 8.0 mm, (b) 8.0 mm > PSR2 > 4.75 mm, and (c) 4.75 mm > PSR3 > 1.35 mm. Error bars represent ± 2 standard deviations ($n = 3$).

for PSR3 and between shorter intervals for PSR1 and PSR2. Maia et al. (2012) recommended that biofilter drying rates should remain in the constant drying region to prevent sharp decreases in removal efficiency. PSR1 remained in the constant drying region for 35% < MC < 50% (approx.), whereas PSR2 remained in the constant drying region for 40% < MC < 60% (approx.). The determination of MC operation ranges in practical applications will increase the efficacy of biofilter moisture control.

EVALUATION OF ISOTHERMS

An analysis was conducted to evaluate whether the isotherms differed by particle size range (table 3) using the Henderson isotherm parameters H_1 and H_2 (eq. 1) obtained from nonlinear regression. Given a regression standard error of about 1.3% of EMC, the four particle size ranges were practically similar (95% C.I.), although the smallest range (PSR3-4) tended to be driest and PSR3-3 tended to be wettest. No significant differences were found between the four particle size ranges for either of the parameters. Therefore, the data were pooled, and a nonlinear regression combining the four particle size ranges was obtained (eq. 4):

$$EMC = [-19.35 \times \ln(1 - ERH)]^{0.6892} \quad (4)$$

The practical implication of this result is that the same EMC can be assumed for the four particle size ranges studied to maintain an equilibrium relative humidity at or above 95%, a reasonable threshold for microbiological activity.

The model applies for $T = 298.15$ K, where ERH is expressed as decimal, $r^2 = 0.945$, model SE = 1.3%, and the SE of H_1 and H_2 are 1.774E-5 and 0.037, respectively. Equation 4 may be used as a reasonable EMC estimator for composted media with this size of particles. Using equation 4, for ERH = 95%, the required minimum moisture to allow microbial activity is 16.41% with absolute uncertainties of $\pm 0.34\%$ (95% confidence interval) and $\pm 2.68\%$ (95% prediction interval). In practical terms, the lowest prediction interval threshold (below about 13.7%) is too dry to support sufficient microbial activity in most microorganisms (Maia et al., 2011a).

AIRFLOW RESISTANCE OF DRY AND WET MEDIA

Tests were run with compost at two low moisture content levels (Dry 1 = 6.8% w.b.; Dry 2 = 5.5% w.b.) and at two high moisture content levels (Wet 1 = 61.9% w.b.; Wet 2 = 64.9% w.b.). A pressure drop as high as 6349.8 Pa m^{-1} was found for airflow of 1461 $m h^{-1}$ and 64.9% w.b. media moisture content, while a pressure drop as low as

Table 4. Pressure drop (PD) along compost column at different moisture contents (MC) and their respective lowest (AVL) and highest (AVH) air velocities; SD = standard deviation.

	MC (% w.b.)	SD	PD-AVH (Pa m^{-1})	AVH ($m h^{-1}$)	PD-AVL (Pa m^{-1})	AVL ($m h^{-1}$)
Dry 1	6.8	0.11	5029.0	1627	101.1	278
Dry 2	5.5	0.01	4694.9	1770	98.1	279
Wet 1	61.9	2.53	6040.3	1570	107.3	59
Wet 2	64.9	2.43	6349.8	1461	113.4	60

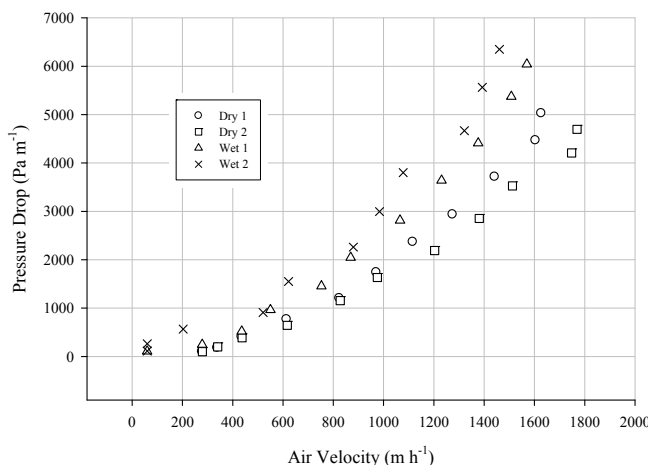


Figure 9. Pressure drop profile at different superficial air velocities and compost moisture contents. Dry 1 and Dry 2 are 6.8% w.b. and 5.5% w.b., respectively. Wet 1 and Wet 2 are 61.9% w.b. and 64.9% w.b., respectively.

98.1 Pa m^{-1} was found for airflow of 279 $m h^{-1}$ and 5.5% w.b. media moisture content (table 4). The values shown in table 4 include the pressure drop across the aeration floor. Flow resistance at different air velocities is shown in figure 9. One can see that pressure drop increases with increased moisture content and air velocity.

The following regression equations were obtained for dry and wet compost:

$$y_{dry} = (0.997 \pm 0.6313)x + (0.0011 \pm 0.0003)x^2 \quad (5)$$

$$y_{wet} = (0.0022 \pm 0.0004)x^2 \quad (6)$$

where y is pressure drop (Pa m^{-1}), and x is superficial air velocity ($m h^{-1}$). Quadratic regression analyses of the dry and wet runs are shown in figure 10. The regression curves provide good association between air velocity and pressure drop ($p < 0.0001$). Static pressures at normalized depths (surface = 0) along the compost column for each run are shown in figure 11. Higher pressure was observed at greater depths and higher air velocities.

Table 3. Parameter values with standard errors and model coefficient of determination associated with equation 4.

Isotherm Model	Parameter ^[a]	Particle Size Range (mm)			
		4.76 < PSR3-1 < 3.36	3.36 < PSR3-2 < 2.28	2.28 < PSR3-3 < 2.00	2.00 < PSR3-4 < 1.68
Henderson ^[b]	$H_1 \pm \Delta H_1$	1.514E-4 a \pm 2.47E-5	1.520E-4 a \pm 2.368E-5	1.455E-4 a \pm 2.275E-5	3.056E-4 a \pm 8.151E-5
	$H_2 \pm \Delta H_2$	1.494 a \pm 0.059	1.495 a \pm 0.056	1.492 a \pm 0.06	1.285 a \pm 0.098
	r^2	0.966	0.968	0.969	0.917
	SE (%)	1.1	1.0	1.0	1.8

^[a] Δ = standard error of the parameter, and SE (%) = standard error of the nonlinear regression.

^[b] Parameter values in the same row followed by different letters are significantly different between particle sizes.

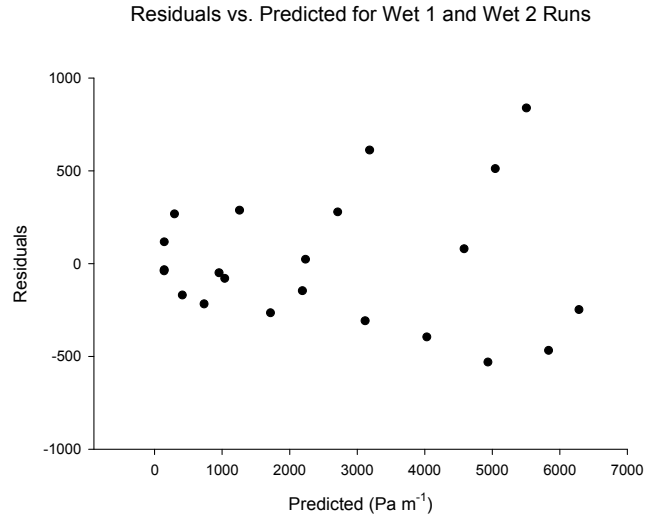
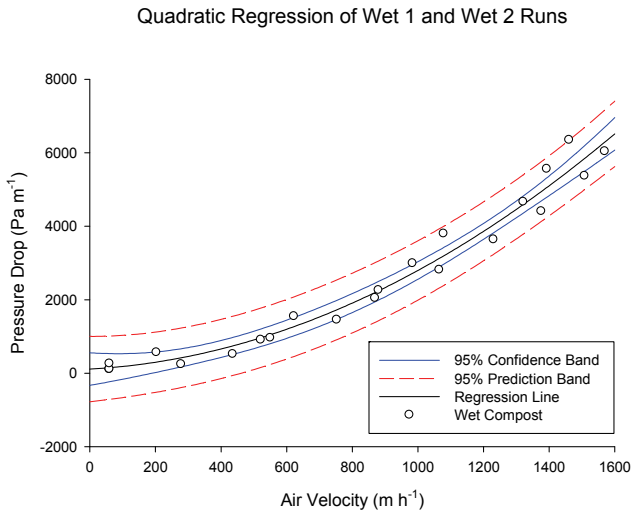
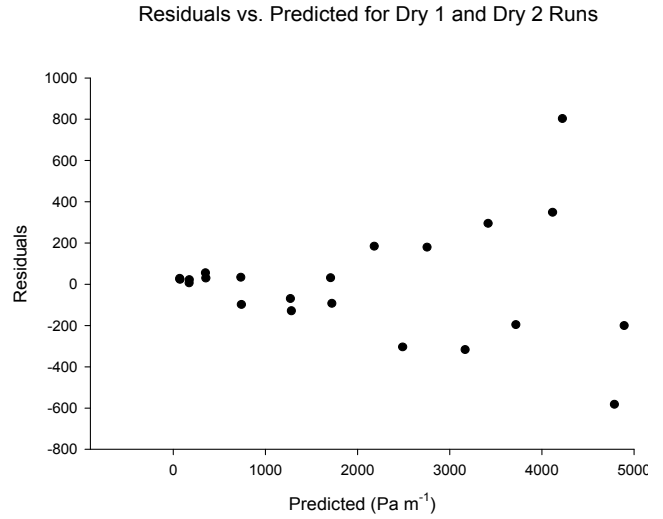
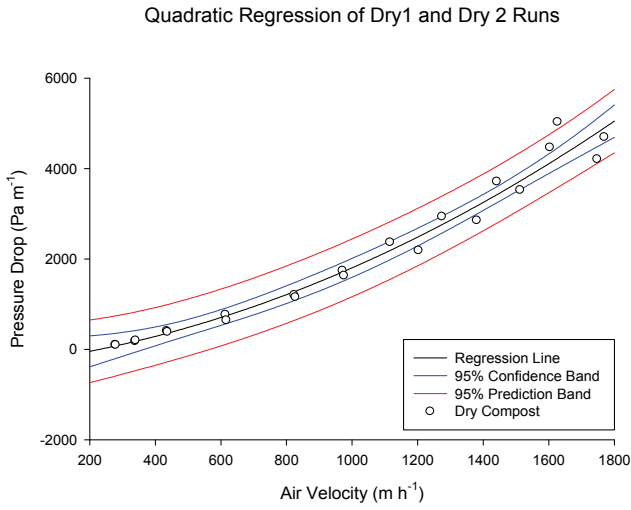
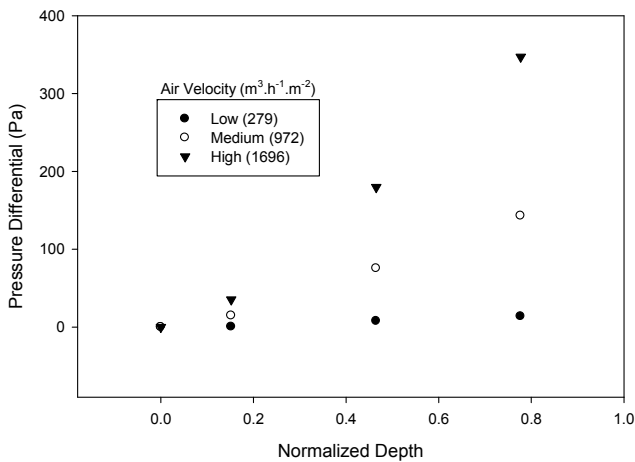


Figure 10. Quadratic regression analysis of runs with dry compost and wet compost.

Resistance to air flow across "dry" compost column (average of "dry 1" and "dry 2")



Resistance to air flow across "wet" compost column (average of "wet 1" and "wet 2")

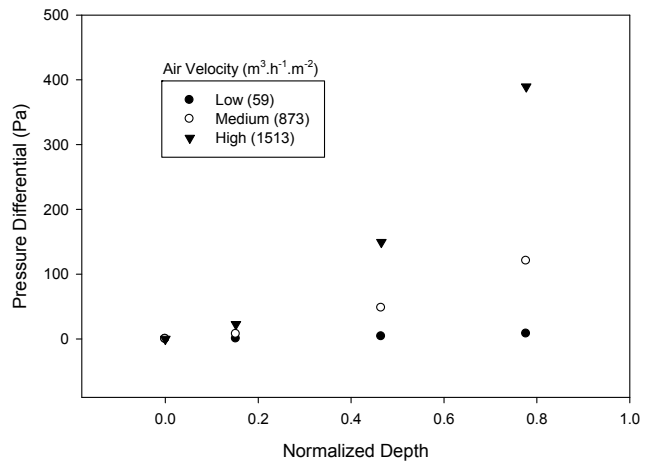


Figure 11. Pressure differences (positive static pressure – atmospheric pressure) at normalized depths of the compost column when dry (left) and wet (right).

SUMMARY OF RESULTS

For the media tested in this study, the following is a summary of results:

Particle size distribution: The largest particle size range (PSR1) comprised $5.5\% \pm 1.1\%$ of the total volume sieved, while the medium particle size range (PSR2) comprised $8.6\% \pm 0.9\%$, and the small particle size range (PSR3) comprised $37.4\% \pm 2.6\%$ of the total volume. Coarser material (>12.5 mm) represented $2.3\% \pm 0.9\%$ and finer material (<1.35 mm) $46.3\% \pm 1.9\%$ of the amount sieved.

Bulk and particle density and porosity: Porosity was reduced for PSR1, PSR2, and PSR3 respectively by 8.4%, 3.2%, and 7.4% of the initial value after compaction at an initial (drier) moisture content of 15.4% to 19.9% w.b. and by 2.4% 1.3%, and 1.9% of the initial value after compaction at 60% w.b. Thus, higher moisture content led to about 2% reduction in porosity after compaction.

Biofilter media field capacity: Considerable range in water-holding capacity among the particle size ranges was noted. PSR1 was able to hold water up to 52.8% w.b. moisture content, while PSR2 and PSR3 held water up to 61.6% w.b. and 72.2% w.b. moisture content, respectively.

Drying rate analysis: The drying rate versus moisture content curve is useful to describe moisture properties of biofilter media for $ERH > 0.99$. PSR1 and PSR2 dried faster than PSR3, reducing drying rate by the 16th day. The constant drying rate stage comprised the moisture range of 34% to 51% w.b. (PSR1), 43% to 61% w.b. (PSR2), and 48% to 71% w.b. (PSR3), represented by abundance of free water. The first falling drying rate stage comprised the moisture range of 27% to 33% w.b. for PSR1 and 39% to 43% w.b. for PSR2. The second falling drying rate stage comprised the range of 5% to 8% w.b. (PSR1) and 8% to 11% w.b. (PSR2).

Water sorption isotherms: There were no significant differences among particle size ranges based on a statistical comparison of the Henderson equation regression coefficients. From the combined pooled parameters for all particle size ranges, to provide $ERH > 95\%$ (a beneficial growth environment for most microbial organisms), the EMC of a mixture of this media must be at or above $16.5\% \pm 2.68\%$ (at 25°C).

Airflow resistance of wet and dry media: A pressure drop as high as 6350 Pa m^{-1} was found for superficial air velocity of 1461 m h^{-1} and $65\% \pm 0.32\%$ w.b. media moisture content, while a pressure drop as low as 98 Pa m^{-1} was found for superficial air velocity of 279 m h^{-1} and $5.5\% \pm 0.01\%$ w.b. media moisture content for the smallest particle size range (PSR3).

CONCLUSIONS AND RECOMMENDATIONS

The development of integrated protocols for physical characterization of gas-phase biofilter media is needed in the technical literature and in the field, owing to the great variability in the composition of materials and their effects on biofilter performance. The selection of media particle size ranges and coarse: fine ratios can directly affect biofilter

operation, with impacts on operation costs caused by changes in pressure drop and potentially the need for additional ventilation equipment (Nicolai and Janni, 2001a, 2001b). Moisture is a key physical parameter, and lack of moisture control is a main cause of biofilter malfunction. Moisture control is critical for maintenance of microbial activity, and it can also significantly affect pressure drop. Moisture and media particle size are fundamentally related; for instance, moisture parameters such as media field capacity and drying rates were shown to be greatly affected by media particle size. In addition to the coarse: fine ratio, moisture also affects bulk density and porosity, and media pressure drop. Media-moisture interactions should be evaluated in-depth using the drying rate versus moisture content curve (for wet media) and the Henderson water-sorption isotherm model (for dry media). These characterizations have the potential to be part of a more comprehensive biofilter operation protocol.

Particle size distribution and porosity: These analyses were performed to characterize the physical composition of organic compost commonly used as gas-phase biofilter medium. While higher porosity portions of compost may be desirable for better aeration of a biofilter, this may not be viable owing to their scarcity compared to lower porosity portions. Thus, the characterization of the material to be used as the biofilter medium may contribute to determining the ideal coarse: fine ratio for a biofiltration system.

Biofilter media field capacity: This analysis should be performed to determine the maximum moisture content held by a gas-phase biofilter. Beyond that point, biofilters do not operate in a gas phase. Field capacity values change for different types of media and within particle size ranges of the same media. Thus, MFC determination should be incorporated as a moisture management tool.

Dry media (isotherms): The use of isotherms to characterize media revealed important properties regarding the minimum moisture levels required to support microbial activity. However, recommendations for optimum media moisture content should be linked to the sorption isotherm behavior of each individual material used as biofilter media. Different candidate materials for gas-phase biofilters may exhibit differing water sorption isotherms, and thus provide opportunities for testing the applicability of the method presented as a biofilter media management tool. The use of the method with different materials, particle size distributions, and porosities is recommended as future work.

Wet media: The drying rate versus moisture content curve was used as a tool to describe the moisture properties of biofilter media for $ERH > 99\%$. The application of this method during biofiltration to determine media moisture conditions is promising, especially for studies testing the effects of different levels of MC on the removal and generation of greenhouse gases, ammonia, and other pollutants of concern. The determination of MC operation ranges in field applications will potentially increase the efficacy of biofilter moisture control.

Airflow resistance of dry and wet media: This analysis provides information regarding a media material's resistance to airflow. Biofilter aeration is essential to enhance contaminant removal efficiency. However, wetter material of the same particle size range increased the airflow re-

sistance by 15.6% to 35.3%. Therefore, assessment of a material's airflow resistance should also take moisture content into consideration, since these two factors are crucial for the balance between operational cost and contaminant removal efficiency of a biofiltration system.

The methods used here are currently being applied in compost bedding characterization for more than 50 dairy barns in Kentucky as part of an on-going extension and research project developed in the Department of Biosystems and Agricultural Engineering of the University of Kentucky.

ACKNOWLEDGEMENTS

This project was conducted with support from USDA-CSREES NRI Air Quality Program.

REFERENCES

- ASHRAE. 1999. ANSI/ASHRAE Standard 51/1999: Laboratory methods of testing fans for aerodynamic performance rating. Atlanta, Ga.: ASHRAE.
- Devinny, S. D., M. A. Deshusses, and T. S. Webster. 1999. *Biofiltration for Air Pollution Control*. 1st ed. Boca Raton, Fla.: Lewis Publishers.
- Dorado, A. D., J. Lafuente, D. Gabriel, and X. Gamisans. 2010. The role of water in the performance of biofilters: Parameterization of pressure drop and sorption for common packing materials. *J. Hazardous Materials* 180(1-3): 693-702.
- Dumont, E., Y. Andr s, P. Le Cloirec, and F. Gaudin. 2008. Evaluation of a new packing material for H₂S removed by biofiltration. *Biochem. Eng. J.* 42(2): 120-127.
- Dutra de Melo, L. 2011. Moisture control methodology for gas-phase compost biofilters. MS thesis. Lexington, Ky.: University of Kentucky, Department of Biosystems and Agricultural Engineering.
- EPA. 2008. Wastes—Resource Conservation—Reduce, Reuse, Recycle—Composting. Washington, D.C.: U.S. Environmental Protection Agency. Available at: www.epa.gov/osw/conserve/rrr/composting/basic.htm. Accessed 7 March 2010.
- Foust, A. S., L. A. Wenzel, C. W. Clump, L. Maus, and L. B. Andersen. 1964. *Principles of Unit Operations*. 1st ed. New York, N.Y.: John Wiley and Sons.
- Funk, T. L., J. M. Appleford, Y. Chen, M. J. Robert, and R. C. Funk. 2005. Moisture sensing methods for biofilters treating exhaust air from livestock buildings. In *Proc. Symposium State of the Science: Animal Manure and Waste Management*. National Center for Manure and Animal Waste Management.
- Henderson, S. M. 1952. A basic concept of equilibrium moisture content. *Agric. Eng.* 33(1): 29-32.
- Henderson, S. M., R. L. Perry, and J. H. Young. 1997. *Principles of Process Engineering*. 4th ed. St. Joseph, Mich.: ASAE.
- Levin, L., L. Villalba, V. Da Re, F. Forchiassin, and L. Papinutti. 2007. Comparative studies of loblolly pine biodegradation and enzyme production by Argentinean white rot fungi focused on biopulping processes. *Proc. Biochem.* 42(6): 995-1002.
- Liberty, K. R. 2002. Yard-waste compost biofilters for ammonia adsorption and biotransformation. PhD diss. Lexington, Ky.: University of Kentucky, Department of Biosystems and Agricultural Engineering.
- Maestre, J. P., X. Gamisans, D. Gabriel, and J. Lafuente. 2007. Fungal biofilters for toluene biofiltration: Evaluation of the performance with four packing materials under different operating conditions. *Chemosphere* 67(4): 684-692.
- Maia, G. D. N. 2010. Ammonia biofiltration and nitrous oxide generation as affected by media moisture content. PhD diss. Lexington, Ky.: University of Kentucky, Department of Biosystems and Agricultural Engineering.
- Maia, G. D. N., G. B. Day V, R. S. Gates, and J. L. Taraba. 2011a. Biofilter media characterization using water sorption isotherms. *Trans. ASABE* 54(4): 1445-1451.
- Maia, G. D. N., G. B. Day V, R. S. Gates, and J. L. Taraba. 2011b. Ammonia biofiltration and nitrous oxide generation during the start-up of gas-phase compost biofilters. *Atmos. Environ.* 46(12): 659-664, doi: 10.1016/j.atmosenv.2011.10.019.
- Maia, G. D. N., G. B. Day V, R. S. Gates, J. Taraba, and M. S. Coyne. 2012. Moisture effects on greenhouse gases generation in nitrifying gas-phase compost biofilters. *Water Research* 46(9): 3023-3031, doi: 10.1016/j.watres.2012.03.007.
- Morgan-Sagastume, M. J., A. Noyola, S. Revah, and J. S. Ergas. 2003. Changes in physical properties of a compost biofilter treating hydrogen sulfide. *J. Air and Waste Mgmt. Assoc.* 53(8): 1011-1021.
- Mujumdar, A. S., and A. S. Menon. 1995. Drying of solids: Principles, classification, and selection of driers. In *Handbook of Industrial Drying*, 1-40. 2nd ed. A. S. Mujumdar, ed. New York, N.Y.: Marcel Dekker.
- Nicolai, R. E., and K. A. Janni. 2001a. Determining pressure drop through compost-woodchip biofilter media. ASAE Paper No. 014080. St. Joseph, Mich.: ASAE.
- Nicolai, R. E., and K. A. Janni. 2001b. Biofilter media mixture ratio of wood chips and compost treating swine odors. *Water Sci. and Tech.* 44(9): 261-267.
- Nicolai, R. E., and R. M. Lefers. 2006. Biofilters used to reduce emissions from livestock housing: A literature review. In *Proc. Workshop on Agricultural Air Quality: State of the Science*, 952-960. V. P. Aneja, W. H. Schlesinger, R. Knighton, G. Jennings, D. Niyogi, W. Gilliam, and C. Duke, eds. Washington, D.C.: USDA-CSREES.
- Nicolai, R. E., and D. Schmidt. 2004. Biofilters. Livestock development in South Dakota: Environment and health. Fact sheet FS 925-C. Brookings, S.D.: South Dakota State University, College of Agriculture and Biological Sciences. Available at: www.sdstate.edu/abe/research/structures/upload/FS925-C.pdf.
- Nicolai R. E., C. J. Clanton, K. A. Janni, and G. L. Malzer. 2006. Ammonia removal during biofiltration as affected by inlet air temperature and media moisture content. *Trans. ASABE* 49(4): 1125-1138.
- Pantoja Filho, J. L. R., L. T. Sader, M. H. R. Z. Damianovic, E. Foresti, and E. L. Silva. 2010. Performance evaluation of packing materials in the removal of hydrogen sulphide in gas-phase biofilters: Polyurethane foam, sugarcane bagasse, and coconut fiber. *Chem. Eng. J.* 158(3): 441-450.
- Pushnov, A. S. 2006. Calculation of average bed porosity. *Chem. and Petroleum Eng.* 42(1-2): 14-17, doi: 10.1007/s10556-006-0045-x.
- Sadaka, S., C. R. Magura, and D. D. Mann. 2002. Vertical and horizontal airflow characteristics of wood/compost mixtures. *Applied Eng. in Agric.* 18(6): 735-741.
- Sales, G. T. 2008. Assessment of biofilter media particle sizes for removing ammonia. MS thesis. Lexington, Ky.: University of Kentucky, Department of Biosystems and Agricultural Engineering.
- Sextstone, A. J., N. P. Revsbech, T. B. Parkin, and J. M. Tiedje. 1985. Direct measurements of oxygen profiles and denitrification rates in soil aggregates. *SSSA J.* 49(3): 645-651.
- USCC. 2002. *Test Methods for the Evaluation of Composting and Compost*. P. B. Leege and W. H. Thompon, eds. Bethesda, Md.: U.S. Composting Council.
- Yang, L., X. Wang, T. L. Funk, and R. S. Gates. 2011. Biofilter media characterization and airflow resistance test. *Trans. ASABE* 54(3): 1127-1136.